THE ASTROPHYSICAL JOURNAL, 203:521–527, 1976 January 15

THE SOLAR SPECTRUM: WAVELENGTHS AND IDENTIFICATIONS FROM 160 TO 770 ANGSTROMS

W. E. BEHRING AND LEONARD COHEN
Laboratory for Solar Physics and Astrophysics, Goddard Space Flight Center
AND
U. FELDMAN* AND G. A. DOSCHEK
E. O. Hulburt Center for Space Research, Naval Research Laboratory
Received 1975 April 14

ABSTRACT

The full-Sun solar spectrum from 160 to 770 Å was photographed under quiet solar conditions by a rocket-borne spectrograph flown in 1973 September. The spectral resolution is 0.06 Å or better. We present a composite list of spectral lines, including wavelengths, identifications, and approximate intensities that were obtained from the present flight and from a previous flight in 1969 May. This line list contains the most accurate solar wavelengths yet obtained in this spectral region. One result is improved energy levels which are given for the two lowest energy configurations of Fe IX through Fe XVI. No detectable relative mass motions of more than 4 km s^{-1} exist between transition zone and coronal regions averaged over the visible disk of the Sun. The wavelengths of emission lines in this spectrum were determined with indicated accuracies ranging between 2 and 20 mÅ. The spectrograph employed a 3 m radius, 600 grooves mm^{-1} gold grating used at grazing incidence.

Subject headings: line identifications — Sun: corona — Sun: spectra — ultraviolet: spectra

I. INTRODUCTION AND EXPERIMENT

A grazing-incidence spectrograph with a spectral resolution of less than 0.06 Å in the wavelength region from 160 to 770 Å was flown to observe the Sun on an Aerobee-200 rocket launched from White Sands Missile Range, New Mexico. The rocket was launched at 1700 UT on 1973 September 21, and reached a peak altitude of 290.6 km. The solar zenith angle was 39°. The solar activity at the time of launch was low. The 8 to 20 Å flux measured by SOLRAD was 3×10^{-3} ergs/cm^2 s.

The spectrograph previously recorded the solar spectrum from 60–385 Å in 1969 May. The results were described by Behring *et al.* (1972) (Paper I), and the spectrograph was described by Behring *et al.* (1973) (Paper II). The instrument uses a 3 m radius concave grating with an angle of incidence of 88°. In order to record spectral lines up to 770 Å for this flight, the previous 1200 line mm^{-1} grating was replaced by a 600 line mm^{-1} gold-coated Bausch and Lomb replica grating blazed at 6° (490 Å). The entrance slit of the instrument was divided into three sections for this flight: an open section 10 mm long at the center of the slit, a short segment (pinhole) 1.2 mm long near the top of the slit, and a section 4.4 mm long near the bottom of the slit that was covered with a 1000 Å thick aluminum filter. The aluminum-filtered spectrum helps in separating lines of different spectral orders. The pinhole spectrum gives some spatial information about the emitting regions along the spectral lines. The spectra were recorded on Kodak 101-05 glass plates.

Other modifications of the instrument were also made for this flight. The slit width was increased to 5 μ from the previous width of 3 μ (1969 flight). Additional light baffles were inserted in the spectrograph, and the secondary slit (see Paper II) was serrated in order to diffuse the scattered light from the secondary slit. We choose the higher altitude Aerobee-200 for this flight rather than the Aerobee-150 in order to increase the effective exposure time. The atmospheric attenuation is appreciably greater at 500–700 Å than at the shorter wavelengths recorded previously. The exposure time for this flight was about 360 s, but because of atmospheric attenuation, the effective exposure time was reduced to 305 s at 200 Å and 234 s at 550 Å. As in the previous flights, the spectrograph was evacuated prior to launch.

The reentry heating problem is significantly greater for the Aerobee-200 rocket than for the Aerobee-150, because of the greater altitudes reached by the Aerobee-200. Because the Ball Brothers biaxial pointing control system contained a section made from magnesium, a coating of FIREX was put on this section to prevent breakup due to weakening by heating during reentry of the rocket. However, on reentry the vaporizing FIREX leaked into the nose cone and produced some chemical fogging of the plates. Because of this, we considerably shortened the development time of the plates. The combined effect of the chemicals and the

* On leave of absence from Tel Aviv University, Tel Aviv, Israel. Work supported in part by a grant from NASA.

short development time produced an uneven development over the plates.

The primary purpose of this paper is to present a wavelength list of solar lines in the ~160–760 Å range that has greater wavelength accuracy than previously published solar spectra. To date, the most accurate wavelengths have been published in Paper I. The wavelength list presented below improves these wavelengths, especially in the 250 Å region. The first order spectral resolution of less than 0.06 Å is sufficiently high to measure profiles of lines. We have previously published some results concerning line profiles obtained from both the 1969 and 1973 flights (Feldman and Behring 1974; Doschek *et al.* 1974).

Since Paper I appeared in print in 1972 July, two more major publications on coronal lines in the same wavelength region were published. The first by Malinovsky and Heroux (1973) gave wavelengths and intensities for the solar spectrum between 50 and 300 Å. Their spectra were measured photoelectrically. The wavelength accuracies were estimated to be better than 0.06 Å, and the full widths at half maximum intensity were approximately 0.25 Å. In the second paper, Firth *et al.* (1974) obtained photographic spectra in the 150–872 Å region from the center of the quiet solar disk and from a region just above the visible limb. Their spectral resolution is ~0.17 Å, and the wavelength errors are ≤0.02 Å. In that paper Firth *et al.* (1974) published a list of about 250 wavelengths, in which all but six of them are various orders of lines with wavelengths shorter than 370 Å. Their wavelengths are compared with a set of wavelengths which are attributed to Fawcett (1974), but which in fact are the wavelengths published in Paper I.

Recently, a summary of the available data on iron and its ions has been given by Reader and Sugar (1975). In their paper they present energy levels for iron ions derived primarily from available laboratory spectra. From our new wavelength list, it is possible to improve some of these energy levels. Therefore, we also present in additional tables improved values for the energy levels of Fe IX through Fe XVI for the $3s^k3p^l$ type configurations.

II. RESULTS AND DISCUSSION

In order to obtain accurate wavelengths from our spectra, it is necessary to have accurate wavelength standards. We chose 10 strong lines from lines of He I, He II, O III, O IV, O V, and Ne VII as primary wavelength standards. The wavelengths of lines of these ions are well known (Kelly and Palumbo 1973). The plates were measured independently a number of times by three different observers on a Grant measuring engine. From these measurements, accurate averaged positions of the lines on the plates were determined. To derive final wavelengths, the 10 primary wavelength standard lines were first used to establish a plate correction curve from approximately 470 to 610 Å. Second, the wavelengths of many lines whose second and third orders fell in this region were approximately determined, and the correction curves were extended over additional wavelength regions. By an iterative procedure which included averaging the wavelengths determined in as many as four orders, the wavelengths of this second group were refined, and the wavelengths of all the remaining lines were determined. Using laboratory spectra, we verified that no detectable wavelength shifts exist between the different spectral orders. Thus all the wavelengths reported in this paper are based entirely on the wavelengths compiled in Kelly and Palumbo (1973) for the 10 strong lines marked in Table 1. In addition, profiles of the lines were obtained from a Grant microdensitometer in order to help determine wavelengths in a few cases that involved blends of lines.

In attempting to determine wavelengths for spectral lines formed by ions in the corona from primary wavelength standards of lines of ions formed in the transition zone, one question that arises is whether or not relative systematic mass motions exist between these different solar atmospheric regions, even when these motions are averaged over the entire Sun. In the event that such motions do exist, the wavelengths of lines formed in the corona would be Doppler-shifted relative to the wavelengths of lines formed in the transition zone. The amount of the shift would depend on the direction of the relative motions, and because the entire Sun was viewed by our spectrograph, the effect would be averaged over shifts at the limb and shifts at the center of the disk. For instance, if the relative mass motion were directed radially outward from the Sun, the Doppler shifts would be a maximum at the center of the disk and zero at the solar limb. We are able to examine this particular case in some detail by using the pinhole spectrum described above and in Paper I. The emission along the lengths of the spectral lines in the pinhole spectrum arises from different regions of the Sun. The emission at the ends of the lines comes from the solar limb, and the emission in the middle of the line comes from the center of the disk. By measuring the spatial separations on the plates between coronal and transition zone lines at different positions along the lengths of the lines in the pinhole spectrum, we are able to determine an upper limit for any net Doppler shifts between the center of the Sun and the solar limb. No statistically significant shifts were measured. The upper limit for relative motion that we obtain in this fashion is 4 km s^{-1}, which at 500 Å corresponds to only 6.7 mÅ. In the wavelength table described below, the wavelengths are derived assuming that no Doppler shift difference exists between lines from the corona and the transition zone.

Wavelengths, identifications, and approximate relative intensities are given for the lines in Table 1. For most of the identified lines the specific transitions are given in Paper I, along with detailed comments on the 1969 spectrum and isoelectronic sequence tables with detailed references. Figure 1 (Plate 14) shows the portion of the spectrum between 400 and 650 Å obtained through the open part of the slit. The lines in Table 1 are taken from both the 1973 flight and the 1969 flight. The lines without intensity estimates were

1976ApJ...203..521B

TABLE 1

SOLAR WAVELENGTHS FROM 160 TO 770 Å

Ion	Solar λ (Å)	Comments	Intensity
Ni XIV	164.13	D	5
	164.18	D	
Ar X	165.49	D	
	165.64	D	
Fe VIII	167.488	C	
Fe VIII	168.170	B	12
Fe VIII	168.546	B	7
Fe VIII	168.929	C WB2X	
	169.614	C	
Ni XIV	169.678	C	
	169.913	C	
Ar X	170.6	E	
	170.8	E	
Fe IX	171.073	B	120
Ni XIV	171.356	C	
	171.532	C	
O V	172.174	C	
O VI	172.934	C	
O VI	173.080	B	
Fe X	174.531	A	100
Fe X	175.263	B	18
Fe X	175.475	C	5
Ni XV	176.690	C W	
	176.980	C	
Fe X	177.239	A	70
S X	177.593	C W	
	177.727	C W	
Fe XI	178.056	B	
	178.720	C	
	178.97	D W	
Ni XV‡	179.265	C	
	179.395	C WB2X	
Fe XI	179.758	C	
Fe XI	180.401	A	120
Fe XI	180.595	C	
Fe XI	181.131	C	3
Fe XI	182.167	A	20
Fe X	182.308	C	3
O VI	183.944	C	
O VI	184.113	C	5
Fe X	184.536	A	30
Fe XI	184.793	C	
Fe VIII, Ni XVI	185.216	B S2X	12
	185.732	C B3X	
Ca XIV	186.605	C	5
S XI	186.84	D	8
Fe XII	186.880	C	17
	186.976	C	
Fe VIII	187.225	C B2X	
Fe XI§	188.216	A	50
	188.299	A	35
	188.493	B	5
S XI	188.667	C	
Ar XI	188.799	C	
	188.997	C	
	189.123	B	5
	189.733	C	
	189.940	C	7
Fe X	190.038	A	9
S XI	190.372	C W	
Fe XII	191.045	C	
Fe XIII, S XI ‡	191.255	C S	5
	191.57	D	
Fe XII	192.394	A	25
	192.630	C	
Fe XI	192.813	B	16
Fe XII	193.509	A	60
	193.715	C	
Ca XIV	193.872	C	
	194.657	C	
	194.803	C W	
Fe XII	195.119	A	90
Fe XIII	196.525	C B2X	4
Fe XII	196.640	C	6
	197.029	C B2X	
Fe XIII	197.434	C	2
	197.847	C W	
S VIII, Fe XII	198.555	C	7
Fe XIII	200.021	B	5
Fe XII, Fe XIII	201.121	B B2X	16
	201.540	C VW	
Fe XII	201.734	C W	
Fe XIII	202.044	A	65
	202.424	C	7
S VIII	202.608	C	
?Fe XI	202.710	C	6
	203.173	C	4
	203.728	B	7
Fe XIII‖	203.793	D	8
Fe XIII	203.826	C B2	19
Fe XIII	204.263	C	
Fe XIII	204.942	B	5
	206.169	C B2X	
	206.253	C	
	206.369	C	
	207.112	C WB2X	
	207.449	B	6
	207.93	D B2X	5
S X	208.322	C	
Fe XIII	208.679	C	
Fe XIII	209.617	C	6
	209.756	C	2
Fe XIII	209.916	B	13
Fe XIV	211.316	B	45
	211.428	C	
Fe XII	211.738	C	
S XII	212.115	C	
	212.34	D	
	213.029	C	
Fe XIII	213.770	B	7
?Fe XII	214.405	C	3
Si VIII	214.76	D	
S XII	215.153	C WB2	
	215.746	C B3X	
Si VIII	216.90	D VWB2	5
Fe IX	217.100	B	10
Fe XII	217.271	C	
S XII	218.179	C W	4
Fe IX*	218.935	C	5
Fe XIV	219.123	B	15
Fe XII	219.438	B	11
Fe XIV	220.082	B	20
	220.247	C	11
	220.870	B	7
S XII	221.410	C	5
Fe XIII	221.822	C	14
	222.993	C W	
	223.202	C W	
Si IX	223.744	C	6
	224.346	C	10
S IX	224.736	B	17
Si IX	225.021	B	24
	225.159	B	14
	225.856	B	8
	226.017	C	2
	226.320	C	10
Si IX	226.998	B	22
Fe XV	227.208	C	
	227.479	C	4
	228.049	C B3X	
S X	228.167	C	11
S IX	228.852	C	5
	229.748	C	

TABLE 1—*Continued*

Ion	Solar λ (Å)	Comments	Intensity
S IX	229.997	C	2
	230.127	C	10
He II	231.444	C	
He II	232.58	D W	4
	233.234	C WB3X	
	233.445	C	3
	233.644	C	3
Fe XV	233.857	C	3
He II	234.356	B B2	15
	235.79	D	
	236.494	C	6
He II	237.333	C W	15
O IV	238.57	D	12
	239.03	D	16
	239.52	D	
	240.394	C	9
Fe XIII	240.713	B B	20
Fe IX*	241.739	B	30
	242.215	C	8
	242.85	D	
He II	243.026	C W	35
	243.42	D	
?Fe XV†	243.790	C	14
	244.16	D	
Fe IX*	244.911	B	20
Fe XIII	246.208	B	20
N IV	247.17	E	3
	247.397	C	8
O V	248.49	D WB2	7
Ni XVII	249.177	C	4
	249.388	C	10
Fe XVI	251.074	C	6
Fe XIII	251.953	B	40
Fe XIV	252.197	B	12
Si X	253.795	B	6
	254.596	B	3
He II	256.320	C	65
Si X#	256.38	D B3X	10
S XIII	256.686	B	20
?Fe XV	256.925	A	20
S X	257.136	C	5
	257.262	A	45
Fe XIV	257.392	A	16
	257.547	C	14
	257.772	B	6
Si IX	258.080	C	5
Si X	258.373	A	50
S X	259.494	B	17
	259.963	C	3
	260.30	D B3X	
Si X	261.056	B	22
	261.731	C	7
Fe XVI	262.984	A	10
S X	264.233	B B3X	20
Fe XIV	264.787	A	50
	270.407	C	5
Fe XIV	270.524	B	35
Si X	271.992	B	18
	272.15	E	
Si VII	272.6	E	
Fe XIV	274.203	B	55
Si VII	275.368	C	11
Si VIII	276.850	C	8
Mg VII	277.042	C	9
Si X	277.265	C	20
Mg VII	278.395	C	7
S XI	281.416	C	7
Fe XV	284.160	B	110
S XI	285.600	C	5
S XI	285.828	C	8
	286.386	C	2
S XII	288.41	D BX	3
Fe XIV	289.160	C	4
	290.710	C S	8
Fe XII	291.010	C	10
Si IX	292.80	D B	15
Si IX	296.123	B	20
	296.22	D	9
Si XI	303.325	A	110
	303.63	D	22
He II	303.782	S VW	500
	304.853	C	4
Fe XI	308.544	B	4
Fe XIII‖	311.552	C	2
Mg VIII	311.77	D B3X	6
Fe XIII‖	312.164	B	8
C IV	312.415	C	3
Mg VIII	313.734	C	11
Si VIII	314.350	C	6
Mg VIII	315.020	C	20
Si VIII	316.216	C	10
Mg VIII	317.01	D	3
Fe XIII	318.14	D	3
Si VIII	319.830	C W	22
Fe XIII‖	320.800	C	7
Fe XV†	327.02	D	2
Al X	332.77	D	13
Fe XIV	334.171	C	30
Fe XVI	335.403	C	60
Fe XII	338.263	C	8
Fe XI	341.112	C	9
Si IX‖	341.949	C	10
Si IX	345.13	D	16
Fe X	345.739	C	11
Fe XII	346.852	C	11
	347.04	D	1
Si X	347.402	C	25
	347.62	D	1
Fe XIII	348.184	C	20
Si IX	349.874	C	20
Fe XII	352.107	C	20
Fe XI	352.670	C	23
Fe XIV	353.833	C	9
Si X	356.038	C	25
	356.114	C	10
Fe XI	356.540	C	6
Fe XI	358.67	D	5
Fe XIII	359.638	C	13
Fe XIII	359.837	B	4
Fe XVI	360.76	D B2X	50
Fe XII	364.468	B	35
Fe X	365.54	D	1
Mg VII	367.668	C	9
Mg IX	368.061	B	100
Fe XI	369.161	C B2X	7
	391.97	D	1
Ne VI	401.14	D	1
Ne VI	401.946	C	9
Ne VI } Mg VI }	403.299	C B2	7
Fe XV†	417.258	C	10
Ca X	419.74	D	3
Mg VIII	430.459	C	11
Mg VII	431.33	D	4
Mg VII	434.932	C B3X	10
Mg VIII	436.728	C	13
	437.14	D	1
Mg IX	444.03	E	1
Mg VII	450.73	D	1
Ne VII	465.219	S	50
Ca IX	466.233	C	2
	476.74	D	4
	477.474	C	5
Si XII	499.405	C	40
O III	507.633	C B2X	9
O III	508.180	S	7
He I	515.57	D B2X	12
Si XII	520.666	C	25
O III	525.795	C B3X	18
He I	537.030	S	30

TABLE 1—*Continued*

Ion	Solar λ (Å)	Comments	Intensity	Ion	Solar λ (Å)	Comments	Intensity
O IV..........	553.333	S	12	O V..........	633.55	D	1
O IV..........	554.076	S B2X	25		641.23	D	3
O IV..........	554.516	S B2X	70		652.707	C	4
O IV..........	555.275	C	8		672.669	C	6
Ca X..........	557.757	C	2		675.70	D	5
Ne VI.........	558.589	C	2	N III..........	685.834	C	5
Ne VI.........	562.827	C B2X	9		700.20	D B2	1
He I..........	584.334	S	140	O III..........	702.975	C VWBX	12
Ar VII........	585.72	D	20	O III..........	703.873	C	14
	589.99	D	1		707.72	D	1
O III..........	599.594	S	12		712.95	D	1
O IV..........	608.404	C	7		718.53	D	4
Mg X } O IV }.......	609.794	B B2	50		719.71	D	1
					739.09	D	1
Mg X.........	624.943	C	25		741.869	C	5
O V..........	629.729	S	130	N IV..........	765.143	C	9

NOTES TO TABLE 1

The first letter in the comment column gives the probable wavelength errors $|\epsilon|$, which are designated by: A, $|\epsilon| < 2$ mÅ; *B*, $|\epsilon| < 4$ mÅ; C, $|\epsilon| < 10$ mÅ; and D, $|\epsilon| < 20$ mÅ. The letter E designates estimated wavelengths of lines too weak to measure. The letter S designates lines used as primary wavelength standards. The remaining part of the comments uses letters with the definitions: W ≡ a wide line; V ≡ very; B ≡ a blend; *n*X ≡ *n*th order(s) line(s); S ≡ a line with a violet component. Examples for interpreting the comments are: B2 ≡ a blend of two lines; B2X ≡ a blend of the line with a second order line.

The intensities are approximate (see text). No intensities are given for lines observed only in the 1969 flight.

* Svensson *et al.* 1974.

† Cowan and Widing 1973.

‡ Fawcett 1974.

§ Behring *et al.* 1972.

‖ From present work; see Table 2.

\# Computed from the Si X multiplet splitting. The wavelength obtained by deconvolution of the blend with He II is 256.42 Å.

observed only in the 1969 flight, either because of the higher solar activity or because of the higher efficiency at shorter wavelengths, of the 1200 groove mm^{-1} grating used. All of these lines fall below 250 Å. The relative intensity estimates of the lines observed in the 1973 flight are only approximate, and should be used with caution. The relative intensities of lines close in wavelength are more accurate, with errors of ±30 percent. We have also given an estimated wavelength accuracy for each line in Table 1. The wavelength errors are divided into four groups: A ≡ <2 mÅ, B ≡ <4 mÅ, C ≡ <10 mÅ, and D ≡ <20 mÅ. These error estimates depend on a number of factors; e.g., the wavelength determination procedure, the intensities of the lines, blending of lines, and plate defects near some lines.

Most of the identifications of the lines in the table were obtained from the compilation of Kelly and Palumbo (1973), except for some recent identifications that were taken from original sources. Finally, some of the identifications are a result of this work. The lines newly classified in this paper are given in Table 2.

TABLE 2

NEW IDENTIFICATIONS

Ion and Transition	λ (Å)
Fe XIII ($3s^23p^2\,{}^3P_2$–$3s^23p3d\,{}^3D_2$)	203.793
Fe XIII ($3s^23p^2\,{}^3P_1$–$3s3p^3\,{}^3P_2$)....................	311.552
Fe XIII ($3s^23p^2\,{}^3P_1$–$3s3p^3\,{}^3P_1$)	312.164
Fe XIII ($3s^23p^2\,{}^3P_2$–$3s3p^3\,{}^3P_2$)....................	320.800
Si IX ($3s^23p^2\,{}^3P_0$–$3s3p^3\,{}^3D_1$)	341.949

As a check on the relative accuracy of the wavelengths in Table 1, we have compared the splittings of the levels of the ions of Fe X, Fe XI, Fe XIII, and Fe XIV, derived from the permitted lines we observe, with the energies corresponding to the forbidden coronal lines of these ions that appear in the visible spectrum. The energies derived from our wavelengths, and the energies derived from the forbidden coronal lines are given in Table 3, along with the differences Δ, or, errors between the energies. The -32 cm^{-1} energy error is larger by $|22|$ cm^{-1} than the expected error. For this reason, we agree with Flower and Nussbaumer (1974) that the ${}^3P_0$–${}^3S_1$ line of Fe XIII (240.713 Å) is probably a blend. Ignoring the -32 cm^{-1} error, we find that the average absolute error is 6.7 cm^{-1}, which corresponds to 4.2 mÅ at 250 Å.

Finally, in Tables 4 to 11 we give improved values for the energy levels of the coronal iron ions. These values were obtained from the wavelengths of the lines given in Table 1. The accuracy of the levels can be judged from the wavelength accuracy given in Table 1 for these lines.

We hope that the wavelength list and energy levels presented in this paper will help in the continuing problem of line identification in laboratory spectra, and will be an aid in the interpretation of the recently obtained Skylab spectra. The wavelengths and energy levels should also be useful for preparations for future efforts such as the Solar Maximum Mission.

We thank James Houston for his excellent assistance in the field and in preparing the instrument for flight.

TABLE 3

COMPARISON BETWEEN GROUND TERM SPLITTINGS AND FORBIDDEN-LINE TRANSITION ENERGIES

Ion	Transition	λ (Å)	σ (cm⁻¹)	Δσ (cm⁻¹)	Forbidden Coronal Line (cm⁻¹)	Δ (cm⁻¹)
Fe x.........	$3s^23p^5\ ^2P_{3/2}-3s3p^6\ ^2S_{1/2}$	345.739	289,236	15,668	15,683	−15
	$^2P_{1/2}\ \ ^2S_{1/2}$	365.54	273,568			
	$^2P_{3/2}-3s^23p^43d\ ^2P_{3/2}$	177.239	564,210	15,688	15,683	+5
	$^2P_{1/2}\ \ ^2P_{3/2}$	182.308	548,522			
	$^2P_{3/2}\ \ ^2S_{1/2}$	184.536	541,900	15,689	15,683	+6
	$^2P_{1/2}\ \ ^2S_{1/2}$	190.038	526,211			
Fe xi........	$3s^23p^4\ ^3P_2-3s3p^5\ ^3P_2$	352.670	283,551	12,666	12,668	−2
	$^3P_1\ \ ^3P_2$	369.161	270,885			
	$^3P_2\ \ ^3P_1$	341.112	293,159	12,686	12,668	+18
	$^3P_1\ \ ^3P_1$	356.540	280,473			
	$^3P_2-3s^23p^33d\ ^3P_2$	188.216	531,304	12,667	12,668	−1
	$^3P_1\ \ ^3P_2$	192.813	518,637			
	$^3P_2\ \ ^3D_2$	178.056	561,621	12,674	12,668	+6
	$^3P_1\ \ ^3D_2$	182.167	548,947			
Fe xiii.......	$3s^23p^2\ ^3P_0-3s3p^3\ ^3D_1$	348.184	287,204	9,300	9,303	−3
	$^3P_1\ \ ^3D_1$	359.837	277,904			
	$^3P_1\ \ ^3P_2$	311.552	320,974	9,253	9,259	−6
	$^3P_2\ \ ^3P_2$	320.800	311,721			
	$^3P_0\ \ ^3S_1$	240.713	415,432	9,271	9,303	−32
	$^3P_1\ \ ^3S_1$	246.208	406,161	9,262	9,259	+3
	$^3P_2\ \ ^3S_1$	251.953	396,899			
	$^3P_1-3s^23p3d\ ^3P_2$	209.617	477,060	9,268	9,259	+9
	$^3P_2\ \ ^3P_2$	213.770	467,792			
	$^3P_0\ \ ^3P_1$	202.044	494,942	18,561	18,561	0
	$^3P_2\ \ ^3P_1$	209.916	476,381			
	$^3P_0\ \ ^3D_1$	197.434	506,498	9,285	9,303	−18
	$^3P_1\ \ ^3D_1$	201.121	497,213	9,270	9,259	+11
	$^3P_2\ \ ^3D_1$	204.942	487,943			
	$^3P_1\ \ ^3D_2$	200.021	499,948	9,254	9,259	−5
	$^3P_2\ \ ^3D_2$	203.793	490,694			
Fe xiv.......	$3s^23p\ \ ^2P_{1/2}-3s3p^2\ ^2S_{1/2}$	274.203	364,693	18,864	18,853	+11
	$^2P_{3/2}\ \ ^2S_{1/2}$	289.160	345,829			
	$^2P_{1/2}\ \ ^2P_{1/2}$	257.392	388,512	18,859	18,853	+6
	$^2P_{3/2}\ \ ^2P_{1/2}$	270.524	369,653			
	$^2P_{1/2}\ \ ^2P_{3/2}$	252.197	396,515	18,853	18,853	0
	$^2P_{3/2}\ \ ^2P_{3/2}$	264.787	377,662			
	$^2P_{1/2}-3s^23d\ ^2D_{3/2}$	211.316	473,225	18,849	18,853	−4
	$^2P_{3/2}\ \ ^2D_{3/2}$	220.082	454,376			

TABLE 4

Fe IX

Configuration	Level	Energy (cm⁻¹)
$3p^6$..........	$^1S_0$	0
$3p^53d$.........	$^3P_1$	408,312
	$^3P_2$	413,669
	$^1D_2$	456,757
	$^3D_1$	460,617
	$^1P_1$	584,546

TABLE 5

Fe X

Configuration	Level	Energy (cm⁻¹)
$3s^23p^5$...............	$^2P_{3/2}$	0
	$^2P_{1/2}$	15,683.2
$3s3p^6$.................	$^2S_{1/2}$	289,236
$3s^23p^4(^1D)3d$..........	$^2S_{1/2}$	541,897
$3s^23p^4(^3P)3d$..........	$^2P_{3/2}$	564,208
	$^2P_{1/2}$	569,882
$3s^23p^4(^3P)3d$..........	$^2D_{5/2}$	572,964
	$^2D_{3/2}$	586,254

TABLE 6

Fe XI

Configuration	Level	Energy (cm⁻¹)
$3s^23p^4$...............	$^3P_2$	0
	$^3P_1$	12,667.9
	$^3P_0$	14,306
$3s3p^5$.................	$^3P_2$	283,551
	$^3P_1$	293,159
$3s^23p^3(X)3d$..........	$^3P_1$	
	$^3P_2$	531,304
$3s^23p^3(^4S)3d$..........	$^3D_3$	554,320
	$^3D_2$	561,618
	$^3D_1$	566,393

TABLE 7

Fe XII

Configuration	Level	Energy (cm⁻¹)
$3s^23p^3$...............	$^4S_{3/2}$	0
$3s3p^4$.................	$^4P_{5/2}$	274,372
	$^4P_{3/2}$	284,005
	$^4P_{1/2}$	288,307
$3s^23p^2(^3P)3d$..........	$^4P_{5/2}$	512,508
	$^4P_{3/2}$	516,772
	$^4P_{1/2}$	519,766

TABLE 8

Fe XIII

Configuration	Level	Energy (cm^{-1})
$3s^23p^2$	$^3P_0$	0
	$^3P_1$	9,302.5
	$^3P_2$	18,561
$3s3p^3$	$^3D_1$	287,205
	$^3D_2$	287,360
	$^3D_3$	
	$^3P_1$	329,647
	$^3P_2$	330,279
	$^3S_1$	415,462
$3s^23p3d$	$^3P_2$	486,358
	$^3P_1$	494,942
	$^3D_1$	506,502
	$^3D_2$	509,250
	$^3D_3$	509,176

TABLE 9

Fe XIV

Configuration	Level	Energy (cm^{-1})
$3s^23p$	$^2P_{1/2}$	0
	$^2P_{3/2}$	18,852.5
$3s3p^2$	$^2D_{3/2}$	299,248
	$^2D_{5/2}$	301,472
	$^2S_{1/2}$	364,693
	$^2P_{1/2}$	388,510
	$^2P_{3/2}$	396,515
$3s^23d$	$^2D_{3/2}$	473,227
	$^2D_{5/2}$	475,217

TABLE 10

Fe XV

Configuration	Level	Energy (cm^{-1})
$3s^2$	$^1S_0$	0
$3s3p$	$^1P_1$	351,914
$3s3d$	$^1D_2$	762,103

TABLE 11

Fe XVI

Configuration	Level	Energy (cm^{-1})
$3s$	$^2S_{1/2}$	0
$3p$	$^2P_{1/2}$	277,190
	$^2P_{3/2}$	298,150
$3d$	$^2D_{3/2}$	675,480
	$^2D_{5/2}$	678,400

We also thank R. J. Ugiansky, who was Project Manager for the flight, and J. Oktavec and J. Poland for precision machining of instrument parts. P. J. Kenny wrote the program for computing the atmospheric attenuation. We would like to express our appreciation to Dr. G. K. Oertel for his assistance and encouragement. Finally, we thank Ball Brothers personnel for preparing the pointing control, and Gunner Briggs and his staff at WSMR for their cooperation and excellence in successfully launching the rocket.

REFERENCES

Behring, W. E., Cohen, Leonard, and Feldman, U. 1972, *Ap. J.*, **175**, 493 (Paper I).
Behring, W. E., Ugiansky, R. J., and Feldman, U. 1973, *Appl. Optics*, **12**, 528 (Paper II).
Cowan, R. D., and Widing, K. 1973, *Ap. J.*, **180**, 285.
Doschek, G. A., Behring, W. E., and Feldman, U. 1974, *Ap. J. (Letters)*, **190**, L141.
Fawcett, B. C. 1974, *Adv. in Atomic Molec. Phys.*, Vol. **10**, (New York: Academic Press), p. 223.
Feldman, U., and Behring, W. E. 1974, *Ap. J. (Letters)*, **189**, L45.
Firth, J. G., Freeman, F. F., Gabriel, A. H., Jones, B. B., Jordan, C., Negus, C. R., Shenton, D. B., and Turner, R. F. 1974, *M.N.R.A.S.*, **166**, 543.
Flower, D. R., and Nussbaumer, H. 1974, *Astr. and Ap.*, **31**, 353.
Kelly, R. L., and Palumbo, L. J. 1973, *NRL Report 7599*, (Washington, D.C.: Naval Research Laboratory).
Malinovsky, M., and Heroux, L. 1973, *Ap. J.*, **181**, 1009.
Reader, J., and Sugar, J. 1975, *J. Phys. Chem. Ref. Data*, Vol. 4, No. 2, p. 353.
Svensson, L. A., Ekberg, J. O., and Edlén, B. 1974, *Solar Phys.*, **34**, 173.

WM. E. BEHRING and LEONARD COHEN: Code 683, Goddard Space Flight Center, Greenbelt, MD 20771

G. A. DOSCHEK and U. FELDMAN: Code 7125.8, E. O. Hulburt Center for Space Research, Naval Research Laboratory, Washington, DC 20375

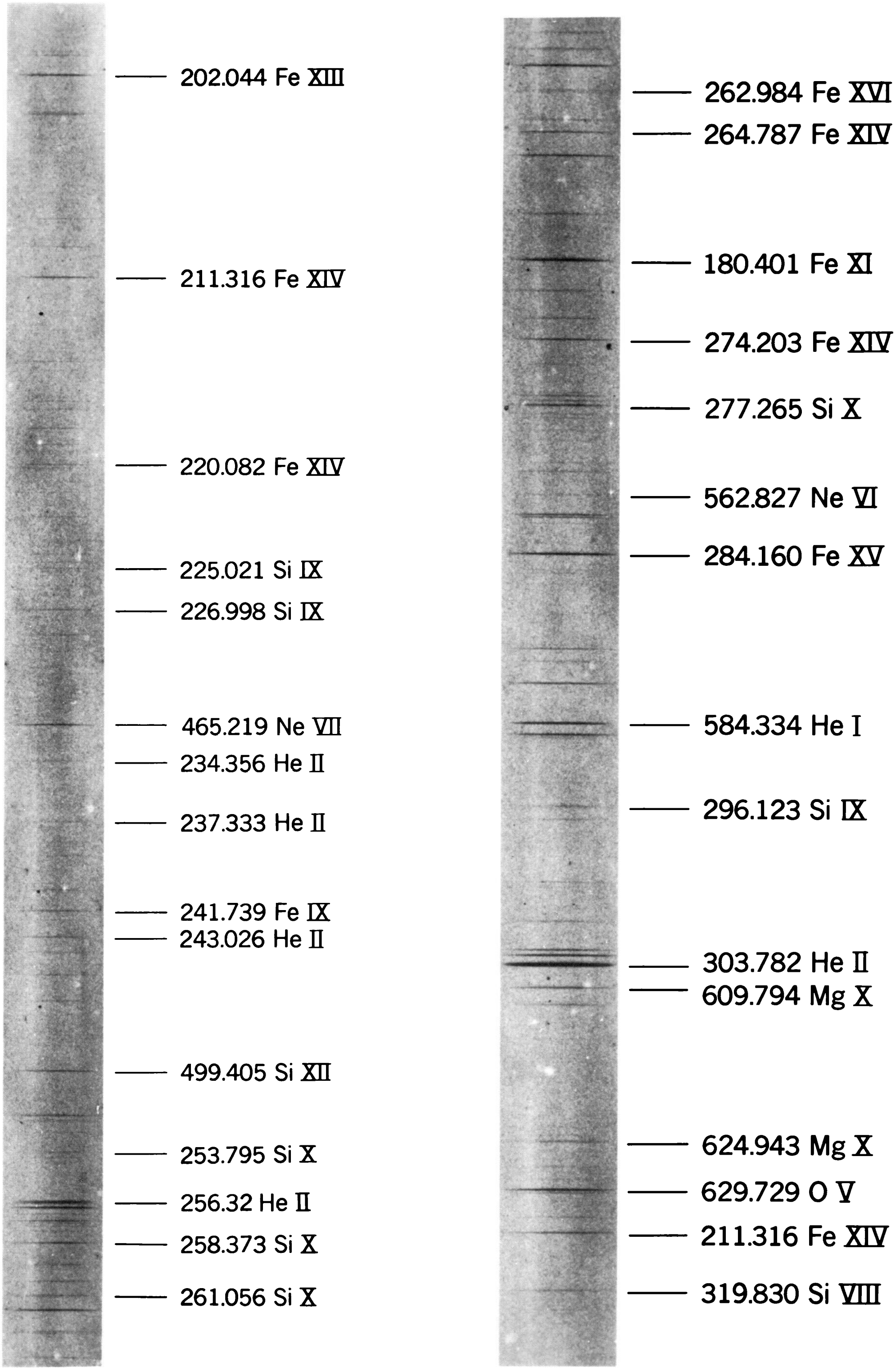

FIG. 1.—A portion of the unfiltered solar spectrum between 400 and 650 Å recorded on 1973 September 21

BEHRING *et al.* (*see* page 522)